EXPERIMENT ON PARAMETER SELECTION OF IMAGE DISTORTION MODEL

Ryuji Matsuoka*, Noboru Sudo, Hideyo Yokotsuka, Mitsuo Sone

Tokai University Research & Information Center
2-28-4 Tomigaya, Shibuya-ku, Tokyo 151-0063, JAPAN
ryuji@yoyogi.ycc.u-tokai.ac.jp, (sdo, yoko)@keyaki.cc.u-tokai.ac.jp, sone3@yoyogi.ycc.u-tokai.ac.jp

Commission V, WG V/1

KEY WORDS: Calibration, Simulation, Camera, Digital, Non-Metric, Distortion, Model, Experiment

ABSTRACT:

Most of current camera calibration methods for a non-metric digital camera adopt polynomials of image coordinates composed of terms representing the correction to the principal distance, the offsets of the principal point, the radial lens distortion, and the decentering lens distortion of the target camera as the image distortion model. However, there is no standard procedure to evaluate appropriateness of parameter selection of the image distortion model. Therefore, we conducted a field experiment on parameter selection of the ordinary image distortion model widely used for camera calibration. We adopted a calibration method using a set of calibration points distributed on the 2-D plane with no ground survey. Four non-metric digital cameras were calibrated in the filed experiment. 16 rounds of camera calibration for six different parameter sets of the image distortion model were conducted. Evaluation of calibration results was performed by differences of image distortions calculated at all pixels on image between the obtained image distortion models. The experiment results indicate that the adoption of the decentering lens distortion component has the significant influence on the estimation of the distribution of image distortion, even if the magnitude of the decentering lens distortion component is small.

1. INTRODUCTION

Many camera calibration methods for a non-metric digital camera have been proposed. Most of them adopt polynomials of image coordinates as the image distortion model. A polynomial image distortion model is generally composed of terms representing the correction to the principal distance, the offsets of the principal point, the radial lens distortion, and the decentering lens distortion of the target camera. Some pieces of calibration software have the function of parameter selection of the image distortion model.

However, there is no standard procedure to evaluate appropriateness of parameter selection of the image distortion model. Furthermore, there are few reports on the influence of the difference of image distortion between the different sets of calibration parameters on the accuracy of 3-D measurement. Consequently, an amateur who would like to calibrate his non-metric digital camera may have difficulty in selecting an appropriate set of calibration parameters.

Accordingly, we conducted a field experiment on parameter selection of the ordinary image distortion model widely used for camera calibration in order to demonstrate the following to an amateur:

(A) How different are image distortion distributions estimated by the different sets of calibration parameters obtained from the same image set?
(B) How large influence on the accuracy of 3-D measurement does the difference of image distortion between the different sets of calibration parameters have?

In this paper, we define the aim of a camera calibration as estimating the distortion distribution of images acquired by the target camera.

2. FIELD EXPERIMENT OF CAMERA CALIBRATION

Most of amateurs would like to use a piece of software that has a calibration function using a 2-D flat sheet with the dedicated pattern (Noma, *et al.*, 2002, Wiggenhagen, 2002, EOS Systems Inc., 2003), because a camera calibration method using 3-D distributed targets is inconvenient and expensive for an amateur to calibrate his digital camera. Therefore, a field experiment of camera calibration was conducted according to our developed calibration method using a set of calibration points distributed on the 2-D plane (Matsuoka, *et al.*, 2003). Our numerical simulation results confirmed that an image distortion model estimated by our method using a set of calibration points on the 2-D plane is expected to be as good as one estimated by a calibration method using a set of calibration points in the 3-D space (Matsuoka, *et al.*, 2005).

2.1 Image Acquisition for Calibration

We prepared a calibration field composed of three by three sheets of approximately 1 m length and 1 m width. Each sheet had ten by ten calibration points placed at intervals of approximately 0.1 m by 0.1 m. Therefore, the calibration field was approximately 3 m long and 3 m wide, and it had 30 by 30 calibration points. Each calibration point was a black filled circle with the radius approximately 11 mm.

A round of camera calibration utilized a set of eight convergent images acquired from eight different directions S1 – S8 with four different camera frame rotation angles of 0° [T], +90° [L], +180° [B] and −90° [R] around the optical axis of the camera as shown in Figure 1. The inclination angle α at image acquisition was approximately 35°.

Four cycles of image acquisition for each camera were executed. 32 images were acquired from eight different directions S1 – S8 with four different camera frame rotation angles [T], [L], [B] and [R] for each cycle of image acquisition. Hence, 128 images were utilized for the calibration of each camera.

2.2 Target Cameras

Four non-metric digital cameras shown in Figure 2 were investigated in the filed experiment. Table 1 shows the specifications of the target cameras. Nikon D1 and Nikon D70 were lens-interchangeable digital SLR (single lens reflex) cameras, Olympus CAMEDIA E-10 was a digital SLR camera equipped with a 4× optical zoom lens, and Canon PowertShot G2 was a digital compact camera equipped with a 3× optical zoom lens. These four cameras are called D1, D70, E-10 and G2 for short from now on. D1 and D70 were calibrated with a 24 mm F2.8 lens, while E-10 and G2 were calibrated at the widest view of their zoom lenses. Hence, they were calibrated with a lens equivalent to around 35 mm in 35 mm film format.

2.3 Image Distortion Model

In the basic image distortion model of this paper, image distortion (Δx, Δy) of a point (x, y) on image is represented as

$$\begin{cases} \Delta x = \Delta x_P + \Delta x_R + \Delta x_D \\ \Delta y = \Delta y_P + \Delta y_R + \Delta y_D \end{cases} \quad (1)$$

$$\begin{cases} \Delta x_R = \bar{x}\left(\dfrac{\Delta c}{c_0} + k_1 r^2 + k_2 r^4 + k_3 r^6\right) \\ \Delta y_R = \bar{y}\left(\dfrac{\Delta c}{c_0} + k_1 r^2 + k_2 r^4 + k_3 r^6\right) \end{cases} \quad (2)$$

$$\begin{cases} \Delta x_D = p_1\left(r^2 + 2\bar{x}^2\right) + 2p_2\bar{x}\bar{y} \\ \Delta y_D = 2p_1\bar{x}\bar{y} + p_2\left(r^2 + 2\bar{y}^2\right) \end{cases} \quad (3)$$

$$\begin{cases} r^2 = \bar{x}^2 + \bar{y}^2 \\ \bar{x} = x - \Delta x_P \\ \bar{y} = y - \Delta y_P \end{cases} \quad (4)$$

where (Δx_P, Δy_P) are the offsets from the principal point to the center of the image frame, (Δx_R, Δy_R) are the radial lens distortion components, and (Δx_D, Δy_D) are the decentering lens distortion components. c_0 is the nominal focal length and Δc is the difference between the calibrated principal distance c and c_0.

Since the basic image distortion model has the radial lens distortion component with the coefficients k_1, k_2 and k_3, and the decentering lens distortion component, the complete parameter set of the model is called R3D in this paper. We examined another five parameter sets R1, R1D, R2, R2D and R3 as shown in Table 2.

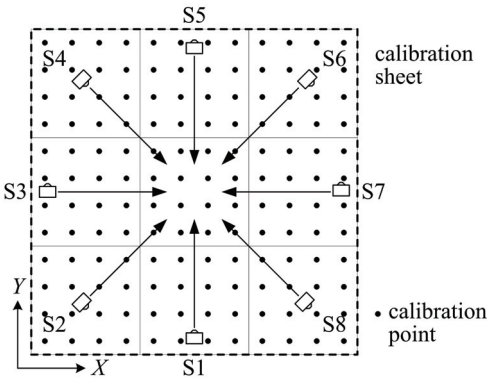

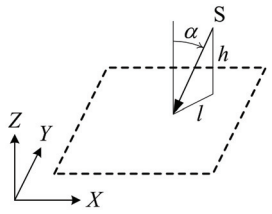

Camera frame rotation angle around the optical axis of the camera at each exposure station as follows:

[T] S1 and S4: 0° (no rotation)
[L] S3 and S6: +90° (left sideways)
[B] S5 and S8: +180° (upside down)
[R] S7 and S2: −90° (right sideways)

Figure 1. Convergent image acquisition from eight different directions

(a) D1 (b) D70 (c) E-10 (d) G2

Figure 2. Target cameras

	Nikon D1	Nikon D70	Olympus CAMEDIA E-10	Canon PowerShot G2
Image sensor	23.7 × 15.6 mm CCD	23.7 × 15.6 mm CCD	Type 2/3 CCD	Type 1/1.8 CCD
Unit cell size in μm	11.8 × 11.8	7.8 × 7.8	3.9 × 3.9	3.125 × 3.125
Recording pixels	2,000 × 1,312	3,008 × 2,000	2,240 × 1,680	2,272 × 1,704
Lens	24 mm F2.8	24 mm F2.8	9 – 36 mm F2 – F2.4	7 – 21 mm F2 – F2.5
35 mm film equivalent	36 mm	36 mm	35 – 140 mm	34 – 102 mm

Table 1. Specifications of the target cameras

Set	Coefficients					
	c	Δx_P Δy_P	k_1	k_2	k_3	p_1 p_2
R1	✓	✓	✓			
R1D	✓	✓	✓			✓
R2	✓	✓	✓	✓		
R2D	✓	✓	✓	✓		✓
R3	✓	✓	✓	✓	✓	
R3D	✓	✓	✓	✓	✓	✓

Table 2. Parameter sets of the image distortion model

2.4 Evaluation Indexes

Some indexes such as V_I, σ_c, (σ_x, σ_y), σ_P, D_T, D_R, D_D and D_P were calculated to evaluate the calibration result.

(A) V_I is root mean squares of residuals on image calculated at the camera calibration.

(B) σ_c is an error estimate of the principal distance c.

(C) (σ_x, σ_y) are error estimates of the offsets (Δx_P, Δy_P) from the principal point to the center of the image frame. σ_P is the absolute value of (σ_x, σ_y), which is calculated using the following equation:

$$\sigma_P = \sqrt{\sigma_x^2 + \sigma_y^2} \tag{5}$$

(D) D_T, D_R and D_D are root mean squares of differences of total image distortions (Δx, Δy), radial lens distortion components (Δx_R, Δy_R) and decentering lens distortion components (Δx_D, Δy_D) calculated at all pixels on image between two obtained image distortion models respectively. These indexes are calculated using the following equations:

$$D_T = \sqrt{\frac{1}{N}\sum_{k=1}^{N}\left\{\left(\Delta x_k^{(T)} - \Delta x_k^{(R)}\right)^2 + \left(\Delta y_k^{(T)} - \Delta y_k^{(R)}\right)^2\right\}} \tag{6}$$

$$D_R = \sqrt{\frac{1}{N}\sum_{k=1}^{N}\left\{\left(\Delta x_{Rk}^{(T)} - \Delta x_{Rk}^{(R)}\right)^2 + \left(\Delta y_{Rk}^{(T)} - \Delta y_{Rk}^{(R)}\right)^2\right\}} \tag{7}$$

$$D_D = \sqrt{\frac{1}{N}\sum_{k=1}^{N}\left\{\left(\Delta x_{Dk}^{(T)} - \Delta x_{Dk}^{(R)}\right)^2 + \left(\Delta y_{Dk}^{(T)} - \Delta y_{Dk}^{(R)}\right)^2\right\}} \tag{8}$$

where N is the number of pixels of the image. Superscripts $^{(T)}$ and $^{(R)}$ indicate two obtained image distortion models, that is to say, the target image distortion model and the reference image distortion model respectively.

(E) D_P is the distance between the estimated principal points of two obtained image distortion models, which is calculated using the following equation:

$$D_P = \sqrt{\left\{\left(\Delta x_P^{(T)} - \Delta x_P^{(R)}\right)^2 + \left(\Delta y_P^{(T)} - \Delta y_P^{(R)}\right)^2\right\}} \tag{9}$$

2.5 Results and Discussion

16 rounds of camera calibration for each parameter set as to each camera were conducted by bundle adjustment with self-calibration. Table 3 shows combinations of eight images utilized in a calibration round from 32 images acquired from eight different directions S1 – S8 with four different camera frame rotation angles of 0° [T], +90° [L], +180° [B] and −90° [R] for a cycle of image acquisition.

Round	S1	S2	S3	S4	S5	S6	S7	S8
1	[T]	[R]	[L]	[T]	[B]	[L]	[R]	[B]
2	[R]	[B]	[T]	[R]	[L]	[T]	[B]	[L]
3	[B]	[L]	[R]	[B]	[T]	[R]	[L]	[T]
4	[L]	[T]	[B]	[L]	[R]	[B]	[T]	[R]

Table 3. Four rounds of camera calibration

The statistics of the camera calibration are as shown in Table 4. Table 4 provides the minimum, maximum and mean values of the number of utilized calibration points, the root mean square V_I of residuals on image, the error estimate σ_c of the principal distance, and the error estimate σ_P of the offset of the principal point.

From the statistics as shown in Table 4, it can be concluded that the parameter sets R1 and R1D are unsuitable for all cameras. As to the other parameter sets R2, R2D, R3 and R3D, it is rather difficult to judge suitableness of a parameter set from the statistics of the camera calibration.

Camera		D1	D70	E-10	G2
Number of calibration points		263 – 295 (281)	275 – 289 (280)	292 – 325 (307)	350 – 386 (371)
RMS V_I of residuals on image (pixels)	R1	0.179 – 0.196 (0.186)	0.262 – 0.279 (0.270)	0.516 – 0.589 (0.555)	0.827 – 0.887 (0.858)
	R1D	0.175 – 0.195 (0.181)	0.256 – 0.273 (0.263)	0.496 – 0.560 (0.531)	0.701 – 0.771 (0.730)
	R2	0.054 – 0.058 (0.056)	0.073 – 0.077 (0.075)	0.141 – 0.151 (0.147)	0.527 – 0.576 (0.555)
	R2D	0.043 – 0.046 (0.044)	0.045 – 0.049 (0.047)	0.062 – 0.075 (0.067)	0.216 – 0.295 (0.251)
	R3	0.054 – 0.057 (0.056)	0.072 – 0.076 (0.074)	0.140 – 0.150 (0.146)	0.527 – 0.576 (0.554)
	R3D	0.042 – 0.045 (0.043)	0.044 – 0.048 (0.046)	0.060 – 0.074 (0.065)	0.210 – 0.292 (0.245)
Error estimate σ_c of the principal distance (μm)	R1	2.579 – 3.129 (2.832)	2.578 – 2.820 (2.693)	2.110 – 2.593 (2.395)	2.315 – 2.571 (2.450)
	R1D	2.522 – 3.048 (2.763)	2.518 – 2.755 (2.629)	2.035 – 2.484 (2.305)	1.963 – 2.233 (2.085)
	R2	0.888 – 1.027 (0.941)	0.788 – 0.847 (0.815)	0.663 – 0.764 (0.718)	1.625 – 1.814 (1.737)
	R2D	0.700 – 0.802 (0.739)	0.488 – 0.546 (0.514)	0.296 – 0.359 (0.329)	0.669 – 0.927 (0.778)
	R3	0.902 – 1.028 (0.952)	0.798 – 0.852 (0.819)	0.685 – 0.779 (0.736)	1.722 – 1.929 (1.833)
	R3D	0.703 – 0.792 (0.740)	0.476 – 0.539 (0.505)	0.297 – 0.361 (0.328)	0.687 – 0.963 (0.806)
Error estimate σ_P of the offset of the principal point (pixels)	R1	0.144 – 0.165 (0.153)	0.211 – 0.225 (0.217)	0.339 – 0.393 (0.368)	0.468 – 0.512 (0.486)
	R1D	0.322 – 0.361 (0.333)	0.464 – 0.491 (0.474)	0.730 – 0.815 (0.774)	0.886 – 0.977 (0.922)
	R2	0.044 – 0.049 (0.046)	0.059 – 0.063 (0.061)	0.092 – 0.102 (0.098)	0.296 – 0.326 (0.315)
	R2D	0.079 – 0.084 (0.081)	0.081 – 0.090 (0.086)	0.092 – 0.111 (0.098)	0.275 – 0.374 (0.318)
	R3	0.044 – 0.048 (0.046)	0.058 – 0.062 (0.060)	0.091 – 0.101 (0.097)	0.296 – 0.327 (0.315)
	R3D	0.077 – 0.082 (0.080)	0.077 – 0.087 (0.082)	0.088 – 0.108 (0.095)	0.267 – 0.370 (0.311)

Table 4. Statistics of the camera calibration [minimum – maximum (mean)]

Table 5 shows the minimum and maximum values of the root mean squares D_T of differences of total image distortions. As to each camera, 256 values of D_T for each combination of the different parameter sets such as R1 and R1D, and 120 values of D_T for each combination of the same parameter sets such as R1 and R1 were calculated by using Equation (6).

The dispersion of the values of D_T shown in Table 5 is larger than that expected from the statistics of the camera calibration shown in Table 4. This fact demonstrates that the statistics of a camera calibration cannot indicate the reliability of the obtained image distortion model.

The values of D_T of the combinations of one of the parameter sets (R1, R2, R3) and one of the parameter sets (R1D, R2D, R3D) were quite large for each camera. This fact indicates that the adoption of the decentering lens distortion component has the significant influence on a calibration result.

The result that the values of D_T of both the combination of R2 and R3, and the combination of R2D and R3D were small enough demonstrates that it is not necessary to adopt the coefficient k_3 of the radial lens distortion component for every target camera.

Hereafter, we focus on the combinations of R1D and R2D, and R2 and R2D. The results of the combination of R1D and R2D will show the influence of the adoption of the coefficient k_2 of the radial lens distortion component, while the results of the combination of R2 and R2D will show the influence of the adoption of the decentering lens distortion component.

D1	R1	R1D	R2	R2D	R3	R3D
R1	0.089 – 1.492					
R1D	1.194 – 3.010	0.091 – 0.998				min. – max.
R2	0.449 – 1.244	1.331 – 2.367	0.030 – 0.410			(pixels)
R2D	1.313 – 2.706	0.496 – 1.316	1.309 – 1.884	0.037 – 0.474		
R3	0.448 – 1.224	1.342 – 2.375	0.013 – 0.416	1.322 – 1.891	0.037 – 0.398	
R3D	1.318 – 2.704	0.488 – 1.293	1.309 – 1.882	0.023 – 0.485	1.322 – 1.889	0.011 – 0.474

D70	R1	R1D	R2	R2D	R3	R3D
R1	0.064 – 0.735					
R1D	2.148 – 3.071	0.070 – 1.502				min. – max.
R2	0.673 – 1.148	2.377 – 3.230	0.022 – 0.235			(pixels)
R2D	2.375 – 2.954	0.655 – 1.346	2.566 – 2.941	0.025 – 0.504		
R3	0.658 – 1.133	2.368 – 3.223	0.028 – 0.250	2.566 – 2.940	0.012 – 0.238	
R3D	2.356 – 2.943	0.644 – 1.324	2.544 – 2.933	0.028 – 0.520	2.544 – 2.932	0.025 – 0.503

E-10	R1	R1D	R2	R2D	R3	R3D
R1	0.098 – 3.598					
R1D	5.260 – 9.437	0.110 – 1.937				min. – max.
R2	1.952 – 3.430	6.270 – 8.631	0.089 – 0.791			(pixels)
R2D	6.982 – 9.557	1.785 – 3.104	7.207 – 8.434	0.103 – 0.946		
R3	1.939 – 3.412	6.275 – 8.636	0.012 – 0.785	7.211 – 8.441	0.090 – 0.771	
R3D	6.940 – 9.556	1.761 – 3.059	7.193 – 8.404	0.029 – 0.972	7.203 – 8.411	0.112 – 0.949

G2	R1	R1D	R2	R2D	R3	R3D
R1	0.395 – 4.802					
R1D	16.993 – 22.109	0.281 – 3.065				min. – max.
R2	1.697 – 6.110	18.533 – 23.296	0.229 – 3.901			(pixels)
R2D	18.156 – 23.385	1.326 – 4.309	19.378 – 24.458	0.156 – 2.684		
R3	1.685 – 6.096	18.523 – 23.283	0.016 – 3.908	19.369 – 24.445	0.221 – 3.896	
R3D	18.132 – 23.376	1.335 – 4.296	19.353 – 24.446	0.060 – 2.690	19.344 – 24.433	0.124 – 2.667

Table 5. Root mean squares D_T of differences of total image distortions [minimum – maximum]

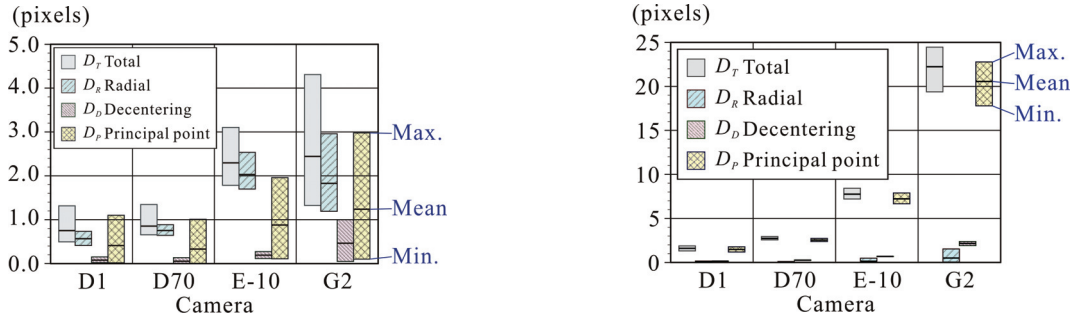

(a) R1D and R2D (b) R2 and R2D

Figure 3. Root mean squares of differences of image distortions

Figure 3 shows the root mean squares D_T, D_R and D_D of differences of total image distortions, radial lens distortion components, and decentering lens distortion components respectively. 256 values of D_T, D_R and D_D for each combination of R1D and R2D, and R2 and R2D were calculated by using Equations (6), (7) and (8) respectively. Moreover, Figure 3 shows the distances D_P between the estimated principal points of two obtained image distortion models calculated by using Equation (9).

The results of the combination of R1D and R2D indicate that the adoption of the coefficient k_2 of the radial lens distortion component has the influence on not only the estimation of the radial lens distortion component but also the determination of the position of the principal point.

On the other hand, the results of the combination of R2 and R2D indicate that the most part of the difference between estimated image distortions was the difference of the estimated position of the principal point, while the differences of another components of the image distortion model were small enough to be negligible. This fact demonstrates that the adoption of the decentering lens distortion component has the significant influence on the estimation of the distribution of image distortion, especially the determination of the position of the principal point, even if the magnitude of the decentering lens distortion component is small.

From the idea that the calibration with no correlation or significantly lower correlation values between parameters is better, some pieces of calibration software have the function that one or more parameters that have high correlations will be removed from the calibration automatically (EOS Systems Inc., 2003). Correlation coefficients between Δx_P and p_1 were found over 0.9 and those between Δy_P and p_2 were found around 0.8 as to R2D in the field experiment. However, the results of the combination of R2 and R2D indicate that the decentering lens distortion component cannot be omitted from the image distortion model.

It is necessary to take notice that the abovementioned results cannot indicate whether an image distortion model such as R2 or R2D is suitable to express image distortion distribution of the target camera or not.

3. SIMULATION OF 3-D MEASUREMENT

A numerical simulation based on the obtained calibration results was conducted in order to investigate the influence of the difference between the obtained image distortion models on the accuracy of 3-D measurement. The reasons that we adopted the numerical simulation were to execute an analysis independent of accuracy of ground coordinates of points, and to control precision of image coordinates.

3.1 Outline of Simulation of 3-D Measurement

Figure 4 shows a sketch of image acquisition for 3-D measurement supposed in the numerical simulation. A pair of convergent images was supposed to be acquired to shoot check points distributed in the 3-D space. Table 6 shows the disposition of control points and check points utilized in the simulation. Eight control points were placed at the vertexes of the cube whose center was at the origin of the *XYZ* ground coordinate system. The disposition of the check points consisted of six layers disposed at regular intervals of the depth (*Z*), and each layer had 100 check points uniformly distributed on the horizontal (*X*-*Y*) plane. Camera positions and attitudes of a pair of images were set up as shown in Table 7. Optical axes of both left and right images intersected each other at the origin of the *XYZ* ground coordinates system.

As to each combination of two parameter sets, 16 data sets were created from 16 calibration results of one parameter set. A round of 3-D measurement was conducted by using one of 16 calibration results of the other parameter set as the given image distortion model, and 16 rounds of 3-D measurement for each data set were conducted. Hence, 256 rounds of 3-D measurement for each combination of two parameter sets were conducted as to each camera.

Two sets of image point data were prepared for each round of 3-D measurement. One was the set that each image coordinate of all control points and check points had no observation error, and the other was the set that random Gaussian errors with 1/6 pixels of standard deviation σ_E ($3\sigma_E$ = 1/2 pixels) were added each image coordinate of all control points and check points. Furthermore, two ways of 3-D measurement were carried out. One was the way that positions and attitudes of the camera used at 3-D measurement were given without an exterior orientation, and the other was the way that positions and attitudes of the camera used at 3-D measurement were unknown and estimated by an exterior orientation by using eight control points.

3.2 Results and Discussion

388, 396, 444, and 462 check points of 600 prepared check points were evaluated in the 3-D measurement simulation of D1, D70, E-10 and G2 respectively.

Figure 5 shows the 3-D measurement errors E_{XY} and E_Z of 256 rounds of the combinations of R1D and R2D, and R2 and R2D. E_{XY} and E_Z are the standard deviations of horizontal and vertical

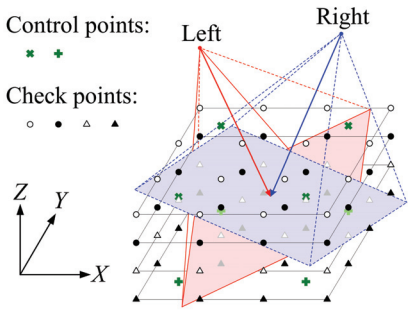

Figure 4. Image acquisition for 3-D measurement

	Control points		Check points		
	Number	Position (m)	Number	Range (m)	Interval (m)
X	2	−0.400, +0.400	10	−0.900 – +0.900	0.200
Y	2	−0.400, +0.400	10	−0.900 – +0.900	0.200
Z	2	−0.400, +0.400	6	−0.500 – +0.500	0.200

Table 6. Dispositions of control points and check points

	X_0 (m)	Y_0 (m)	Z_0 (m)	ω (rad)	ϕ (rad)	κ (rad)
Left	−1.000	0.000	+2.000	0.000	$+\tan^{-1}(1/2)$	0.000
Right	+1.000	0.000	+2.000	0.000	$-\tan^{-1}(1/2)$	0.000

Table 7. Camera positions and attitudes

relative errors of check points respectively, and those were calculated using the following equation:

$$\begin{cases} E_{XY} = \sqrt{\frac{1}{n}\sum_{i=1}^{n}\left\{\frac{\left(e_{Xi}^2 + e_{Yi}^2\right)^{1/2}}{H - Z_i}\right\}^2} \\ E_Z = \sqrt{\frac{1}{n}\sum_{i=1}^{n}\left(\frac{e_{Zi}}{H - Z_i}\right)^2} \end{cases} \quad (10)$$

where (e_{Xi}, e_{Yi}, e_{Zi}) is the 3-D measurement error of the check point i (X_i, Y_i, Z_i), n is the number of check points, and H is the average camera height (2 m) of the two images. The unit ‰ (per mill) in Figure 5 means 10^{-3}.

As to 3-D measurement without an exterior orientation, the difference of image distortion between the different parameter sets had a significant influence on the accuracy of 3-D measurement.

On the contrary, the case was different with 3-D measurement with an exterior orientation. The influence of the difference of image distortion between the different parameter sets on the accuracy of 3-D measurement with an exterior orientation was rather small for every camera, even though the difference of image distortion was large.

4. CONCLUSION

The experiment results indicate that the adoption of the decentering lens distortion component has the significant influence on the estimation of the distribution of image distortion, even if the magnitude of the decentering lens distortion component is small. On the other hand, from the experiment results it can be concluded that it is not necessary to adopt the coefficient k_3 of the radial lens distortion component for the target cameras.

The difference of image distortion between the different parameter sets of the image distortion model had a significant influence on the accuracy of 3-D measurement without an exterior orientation. On the contrary, as to 3-D measurement with an exterior orientation, the influence of the difference of image distortion between the different parameter sets on the accuracy of 3-D measurement was rather small for every camera, even though the difference of image distortion was large.

REFERENCES

EOS Systems Inc., 2003. PhotoModeler Pro 5 User Manual, Vancouver.

Matsuoka, R., Fukue, K., Cho, K., Shimoda, H., Matsumae, Y., 2003. A New Calibration System of a Non-Metric Digital Camera, *Optical 3-D Measurement Techniques VI*, Vol. I, pp. 130 – 137.

Matsuoka, R., Fukue, K., Sone, M., Sudo, N., Yokotsuka, H., 2005. A Study on Effectiveness of Control Points on the 2D plane for Calibration of Non-metric Camera, *Journal of the Japan Society of Photogrammetry and Remote Sensing*, Vol. 43, No. 6, pp. 34 – 47. (in Japanese)

Noma, T., Otani, H., Ito, T., Yamada M., Kochi, N., 2002. New System of Digital Camera Calibration, DC-1000, *The International Archives of the Photogrammetry, Remote Sensing and Spatial Information Sciences*, Vol. XXXIV, Part 5, pp. 54 – 59.

Wiggenhagen, M., 2002. Calibration of Digital Consumer Cameras for Photogrammetric Applications, *The International Archives of the Photogrammetry, Remote Sensing and Spatial Information Sciences*, Vol. XXXIV, Part 3B, pp. 301 – 304.

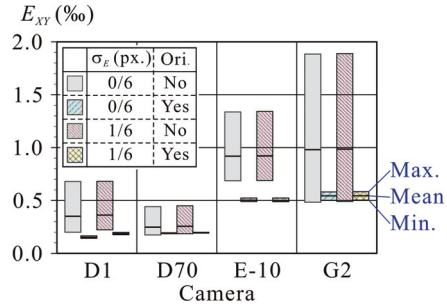

(a) [R1D vs. R2D] Horizontal relative errors E_{XY}

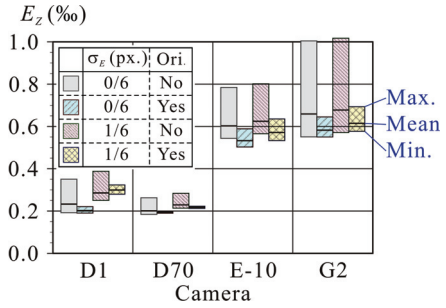

(b) [R1D vs. R2D] Vertical relative errors E_Z

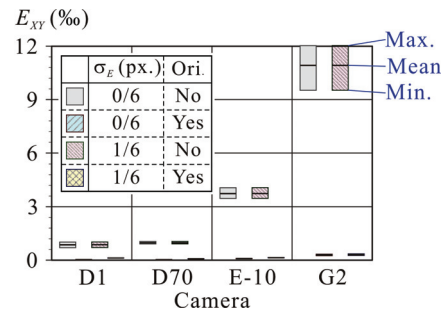

(c) [R2 vs. R2D] Horizontal relative errors E_{XY}

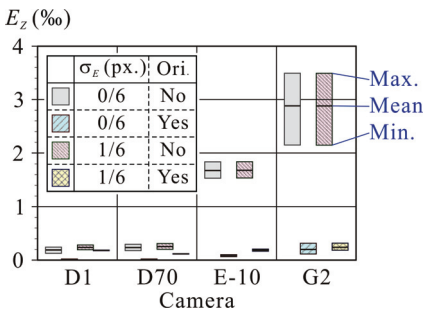

(d) [R2 vs. R2D] Vertical relative errors E_Z

Figure 5. 3-D measurement errors for combination of the different models